723

GHOST STOCHASTIC RESONANCE FOR A STOCHASTIC SINGLE NEURON MODEL

Maria Teresa Giraudo and Laura sacerdote

Abstract. The response of a neuron to a linear combination of the first two harmonics of a fundamental frequency is studied by means of a leaky integrate and fire model. A suitable modification of the classical stochastic model is introduced to consider such input. The resulting interspike interval distribution exhibits maxima in correspondence with the fundamental frequency that was absent in the input signal. This fact shows the ability of the system to recognize the "ghost" frequency. Resonance-like behavior is also showed by the model neuron in a set of instances. The simplicity of the considered model makes also easy to understand the features involved in the ghost resonance phenomenon and to recognize the parameter the ranges compatible with such behavior.

1 Introduction Much effort has been devoted in literature to describe the response of neurons to simple input signals, usually harmonic ones. However only a few studies consider the response to multiple stimuli such as the superposition of one or more periodic terms. Signals of this type arise for example when acoustic perception problems are under examinationin or in diagnostics, as in the analysis of evoked potentials in the human visual cortex (Visual and Conte (2000)). Moreover, it is also known that complex sounds are perceived when the (two) constituent tones are presented binaurally, i.e. one for each ear.

These problems have been treated recently in literature either for neuronal models based on very simple noisy threshold devices (Chialvo et al. (2002), Chialvo (2003)) or for stochastic Morris-Lecar neuronal models (Balenzuela and Garcia-Ojalvo (2005)). In this last case the response of small neural networks to a linear combination of two in-phase harmonic signals, each driven by a different noisy neuron sending pulses to a third one, has also been studied. The output of the models appears to detect a frequency which is absent in the original input signal. Indeed the normalized count plots of the interspike interval (ISI) distributions show a multimodal shape with peaks centered around the fundamental frequency or its multiples. This frequency is recognized as the "missing fundamental" or "ghost" frequency. Such fundamental frequency, which is lacking in the input, is thus nevertheless perceived by the system. Moreover similarly to the case with a single modulation frequency the quoted systems also exhibit a resonance-like behavior (cf. for example Segundo et al. (1994), Kitajo et al. (2003), Wenning and Obermayer (2003)) in correspondence with the ghost frequency for specific ranges of the noise. The analysis performed in Chialvo et al. (2002), Chialvo (2003) and Balenzuela and Garcia-Ojalvo (2005) show that the models respond optimally to the missing fundamental of the harmonic complex signal for an intermediate level of noise. The same behavior, that has been denoted as "ghost resonance", has been replicated experimentally in other nonlinear systems such as semiconductor devices (Buldù et al. (2003)) or electronic circuits (Calvo and Chialvo (2005)).

Our aim is to reinterpret the problems exposed above employing a stochastic leaky integrate and fire model (LIFM) to describe the time course of the neuron membrane potential. The stochastic LIFM is a stochastic threshold model whose validity for the description of the membrane potential behavior in a series of conditions is generally accepted (cf. for example Tuckwell (1988)). It retains the main physiological features of the neuronal cell membrane potential such as the spontaneous decay in the absence of stimuli and it is sufficiently simple to allow the detection of the most relevant phenomena. We are concerned here with the response of such model neuron to stimuli composed with the sum of two successive harmonics of the same fundamental frequency to recognize if it detects the missing frequency and to investigate on the possible arising of ghost resonance phenomena. The simplicity of the considered stochastic model for single neuron activity can facilitate the understanding of leading paradigms involved in time spiking activity and the analysis of related phenomena such as the synchronization between different neurons.

In Section 2 we introduce the model together with the methods employed to study the effects of the above mentioned stimuli. Our results are illustrated by means of some examples in Section 3. We conclude in Section 4 with a brief discussion of the results.

2   Model and Methods The classical stochastic LIFM describes the underthreshold time course of the membrane potential X_t as solution to the following stochastic differential equation (SDE):

$$dX_t = \left(-\frac{X_t}{\theta} + \mu\right) dt + \sigma dW_t; \tag{1}$$

$$X_0 = x_0.$$

Here μ and $\sigma^2 > 0$ are constants representing respectively the net input and the noise amplitude, θ is the membrane time constant and W_t is a standard Wiener process. Without loss of generality we always fix $x_0 = 0\,mV$ since this simply implies a shift with respect to any other value. The advantages of this model reside in the fact that it retains the decay of the membrane potential while the intrinsic nonlinearity of the spiking activity is captured by a threshold mechanism. The process X_t is the well known Ornstein-Uhlenbeck (O.-U.) diffusion process (cf. for example Ricciardi et al. (1999)) which is characterized by linear drift and constant infinitesimal variance.

For model (1) one assumes that a spike is elicited at the time when the stochastic process X_t first reaches a given constant spiking threshold S. After each spike the membrane potential is instantaneously reset to its resting value, set for simplicity to $X_0 = 0\,mV$. The ISIs have then their mathematical counterpart in the first passage time (FPT) random variable

$$T = \inf\left\{t \geq 0 : X_t \geq S; X_0 = 0 < S\right\}. \tag{2}$$

It is possible in this case to define a FPT probability density function $g(t)$ as

$$g(t) = \frac{\partial}{\partial t} P\left(T \leq t\right). \tag{3}$$

Some variations over model (1) are treated for example in Bulsara et al. (1996) and in Shimokawa et al. (1999) where external inputs are introduced. These studies performed on the stochastic LIFM with an additional periodic term in the drift coefficient show that it exhibits a stochastic resonance-like behavior. Indeed the response of the system to even feeble input information results to be amplified and optimized due to the presence of noise.

Here we consider a further modification of the stochastic LIFM where a linear combination of two periodic signals with different frequencies f_1 and f_2 is added to the drift

coefficient. Denoting as f_0 the fundamental frequency we put in particular $f_1 = 2f_0$ and $f_2 = 3f_0$, thus considering the first two harmonics of the fundamental frequency. The resulting process X_t is then solution to the following SDE:

$$(4) \qquad dX_t = \left(-\frac{X_t}{\theta} + \mu + A \left(cos\left(f_1 t + \phi_1 \right) + cos\left(f_2 t + \phi_2 \right) \right) \right) dt + \sigma dW_t;$$

$$X_0 = 0$$

In eq. (4) the parameters μ, σ^2 and θ preserve the same meaning as in eq. (1), A is the constant modulation amplitude and ϕ_1, ϕ_2 are the initial phases of the two modulation components, that are both set equal to 0 in our model.

As far as the modulation phases are concerned two alternative approaches can be followed, contemplating either their resetting after each spike or the uninterrupted evolving of the input signal. While we refer to Lánský (1997) for a detailed discussion on the subject, we follow here both approaches. If the modulation phases are reset to their initial (null) value after each spike a FPT random variable as in (2) is introduced to describe the ISIs. The series of ISIs $\{T_1, T_2, ..., T_k, ...\}$ can then be viewed as a series of event times from a renewal process. In the case where the time course of the input modulation is not stopped after each spike the ISI series can no longer be considered as generated by a renewal process and a FPT density cannot be defined. The series of ISIs $\{T_1, T_2, ..., T_k, ...\}$ gives then rise to a time series.

To understand the response of the model neuron described by eq. (4) to the compound stimulus we can distinguish among two different settings:

(a): the case of $\sigma^2 = 0 \, mV^2 msec^{-1}$, corresponding to the deterministic regime;

(b): the case of $\sigma^2 > 0 \, mV^2 msec^{-1}$, corresponding to the stochastic regime.

(a): *Deterministic regime.* The closed form solution to eq. (4) can be explicitly evaluated (cf. for example Arnold (1974)). We first address the instance where the modulation phases are reset to the values $\phi_1 = 0, \phi_2 = 0$ after each threshold crossing. Defining

$$(5) \qquad\qquad a(t) = A \left(cos\left(f_1 t \right) + cos\left(f_2 t \right) \right)$$

one has

$$(6) \qquad\qquad X_t = F(t) \int_0^t F^{-1}(s) a(s) ds$$

where $F(t)$ is the fundamental solution to the equation

$$(7) \qquad\qquad \frac{dF(t)}{dt} = -\frac{1}{\theta} F(t).$$

¿From (6) and (7) one then easily obtains

$$(8) \qquad X_t = A\theta \left(\frac{1}{1 + f_1^2 \theta^2} \left(cos\left(f_1 t \right) + f_1 \theta sin\left(f_1 t \right) - e^{-\frac{t}{\theta}} \right) \right.$$

$$\left. + \frac{1}{1 + f_2^2 \theta^2} \left(cos\left(f_2 t \right) + f_2 \theta sin\left(f_2 t \right) - e^{-\frac{t}{\theta}} \right) \right) + \mu\theta \left(1 - e^{-\frac{t}{\theta}} \right).$$

The suprathreshold regime corresponds in this case to fulfilling the condition

$$(9) \qquad\qquad \max\{X_t\} = \theta \left(\mu + A \left[\frac{1}{\sqrt{1 + f_1^2 \theta^2}} + \frac{1}{\sqrt{1 + f_2^2 \theta^2}} \right] \right) \geq S.$$

When the stimulus phases are not reset after the occurrence of a spike eq. (8) describes the behavior of the membrane potential only up to the time T_1 when the first spike occurs. The membrane potential behavior is then described by the function

$$
\begin{aligned}
X_t^{(i)} = A\theta \Bigg[& \frac{1}{1+f_1^2\theta^2} \left(\cos(f_1\,(t+T_i)) + f_1\theta\sin(f_1\,(t+T_i))\right) \\
& - \left(\cos\left(f_1 T_i\right) + f_1\theta\sin\left(f_1 T_i\right)\right) e^{-\frac{t}{\theta}}\Bigg) \\
& + \frac{1}{1+f_2^2\theta^2} \left(\cos(f_2\,(t+T_i)) + f_2\theta\sin(f_2\,(t+T_i))\right) \\
& - \left(\cos\left(f_2 T_i\right) + f_2\theta\sin\left(f_2 T_i\right)\right) e^{-\frac{t}{\theta}}\Bigg)\Bigg] + \mu\theta\left(1 - e^{-\frac{t}{\theta}}\right)
\end{aligned}
$$

(10)

for $t \in [T_i, T_{i+1}]$, $i = 1, 2, ..., k, ...$.

(b): *Stochastic regime.* When the system (4) is characterized by a not null noise level and a phase reset is performed after each spike the deterministic solution (8) can be read as the behavior of the mean value of the membrane potential, $\mathbb{E}[X_t]$. A similar role is played by the solution (10) for the case without phase resetting. However in this case one should condition the solutions $X_t^{(i)}$ to belong to the random intervals $[T_i, T_{i+1}]$, $i = 1, 2, ..., k, ...$. Some insight on the ISI distribution in the presence of noise can be got by considering the crossings of the mean membrane potential $\mathbb{E}[X_t]$ happening in the strip $\mathbb{E}[X_t]\pm\sqrt{Var[X_t]}$, where $Var[X_t]$ denotes the variance of the diffusion process X_t. For the considered model we have (cf. Arnold (1974))

$$
(11) \qquad\qquad Var[X_t] = \frac{\sigma^2\theta}{2}\left(1 - e^{-\frac{t}{\theta}}\right).
$$

The fluctuations within the above mentioned strip make crossings allowable even in the underthreshold regime.

Also in the stochastic regime (b) we consider the distribution of the ISIs distinguishing between instances where the modulation phases are reset or not after each spike. The study is performed via computer simulation of the firing times. By suitably transforming the FPT problem for the model described by (4) through a constant threshold into the corresponding problem for the O.-U. process through an oscillating threshold the numerical procedure proposed in Buonocore et al. (1987) could be employed to compute the FPT probability density function (3) in the case where the stimulus phases are reset after the spikes. However, since the same procedure cannot allow to obtain the ISI distribution in the case without phase resetting, it becomes necessary to resort to simulation techniques and the use of the same methodology for the two instances with and without phase resetting appears to be more coherent. We employ an algorithm which is a modification of the method proposed in Giraudo and Sacerdote (1999) for first passage times through boundaries of diffusion processes. The method allows to enhance the reliability of the simulation of FPT's for time homogeneous diffusion processes by suitably evaluating the probability of crossing the threshold in each time discretization interval. Since the process described by (4) is not time homogeneous we adopt a slight modification of the algorithm by freezing the values of the drift in eq. (4) at the initial point of each time discretization interval. We then determine the crossing probabilities of the corresponding tied-down process that, in analogy with what is done in Giraudo and Sacerdote (1999), are used to account for possible exits occurred inside each time discretizaton interval. For every case examined $N = 40000$ simulation runs are executed. When the stimulus phases are reset after each spike we can approximate the FPT density (3) by means of the histograms of simulated interspike intervals. In the case

where no phase reset is performed we employ normalized count plots to represent the ISI distribution. The use of histograms or of normalized count plots allows to recognize the detection of the ghost frequency by the model and the possible arising of resonance-like phenomena. To estimate the coherence of the output with the frequencies of interest we analyze whether corresponding peaks arise in the histograms or normalized count plots. Stochastic resonance can be recognized by studying whether the ISI densities height at the modulation period goes through a maximum when the noise intensity σ^2 is varied while keeping all the other parameters of the model fixed. Hence we look at the height of the peaks at the period $T_0 = \frac{2\pi}{f_0}$ corresponding to the fundamental frequency f_0. Moreover we compute also the fraction of ISIs that fall in the time interval $T_0 \pm 5\%$ by simply dividing the number of those that satisfy such condition by the total number of simulated ISIs.

3   Examples To investigate on the role of the superposition of two harmonic input signals on the ISI distribution for model (4) we consider here some examples distinguishing between the fully deterministic case **(a)** and the stochastic one **(b)**. We always consider both instances where the modulation phase is reset or not after each occurrence of a spike.

In all the Figures we always represent in the left-hand and right-hand panels respectively the results obtained resetting or not the modulation phases after the spikes.

While in case **(a)** we choose the suprathreshold regime to better show the dynamics of the membrane potential X_t, in case **(b)** we remain in the subthreshold regime to study the effects of the noise component since its behavior in the suprathreshold regime is known from the analogous deterministic case. This implies to fulfill the constraint

$$(12) \qquad\qquad \max\{\mathbb{E}[X_t]\} < S.$$

To obtain mean firing frequencies for the original stochastic LIFM lying between 5 and 30 spikes per second, which is generally considered as reasonable, further constraints for the parameter values must be satisfied. Here we compute the mean firing frequency as the inverse of the mean ISI, though different definitions for the mean firing frequency can be given (cf. Lánský et al. (2004)).

We restrict our study to the case where $\mu > 0$ to avoid the occurrence of long tails in the ISI distribution. A preliminary study shows that too small values for the amplitude A do not allow the system to perceive the modulation, hence we limit ourselves to consider cases where $A \geq 0.5\,mV\,msec^{-1}$. The best coherence between input and output signal is expected when the ISI distribution mode is approximately near the period T_0. Indeed the detection of T_0 in this case is facilitated by the higher probability of spiking around such value in the absence of additional stimuli. This leads us in the choice of the range for the noise level σ^2.

We then consider as a reference case the one characterized by fixed $S = 10\,mV$, $\theta = 10\,msec$, $\mu = 0.6\,mV\,msec^{-1}$ and we vary the values of f_0, A and σ^2 as required by the different criteria of analysis chosen.

Case (a). In Fig. 1, panels a and b respectively, we show the behavior of the membrane potential X_t given by eq. (8) and (10) when $A = 1.5\,mV\,msec^{-1}$ and $f_0 = 0.28559\,msec^{-1}$.

It can be clearly detected that after a short onset regime the firing times are regularly spaced at intervals equal to T_0 in the case with reset (panel a), while different values of the initial phases in the stimulus (panel b) can determine the skipping of spiking times at multiples of T_0. Note that the solution (8) is asymptotically periodic with period T_0. In the case considered we have $T_0 \simeq 22\,msec$.

Case (b). We consider now the case where $\sigma^2 > 0\,mV^2msec^{-1}$. With the aim of establishing the role of the different parameters on the response of the system to the composed modulation we consider two different frameworks:
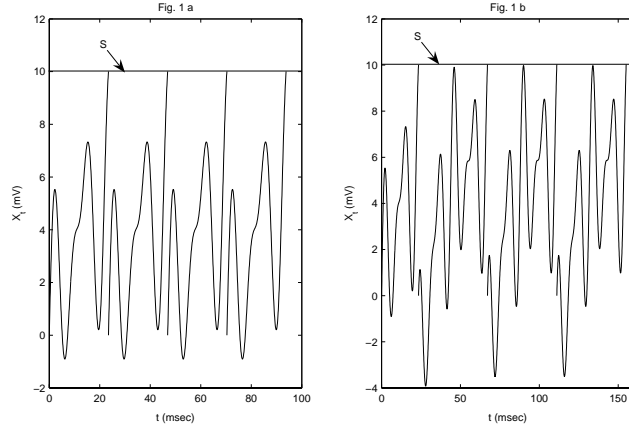
Figure 1: Plot of eq. (8) and (10), panels a and b respectively, for $S = 10\,mV$, $\theta = 10\,msec$, $\mu = 0.6\,mV\,msec^{-1}$, $A = 1.5\,mV\,msec^{-1}$ and $f_0 = 0.28559\,msec^{-1}$.

($\mathbf{1}$) : for fixed S, θ, μ and f_0 we let the modulation amplitude A vary;

($\mathbf{2}$) : for fixed S, θ, μ and A we let the modulation fundamental frequency f_0 vary.

Framework ($\mathbf{1}$). We compare in Fig. 2 the simulated ISI distributions for the same set of parameter values as for Fig. 1, but for $f_0 = 0.196349\,msec^{-1}$, $\sigma^2 = 0.9\,mV^2msec^{-1}$ and smaller values of the amplitude A ($0.5\,mV\,msec^{-1}$, upper panels, and $0.9\,mV\,msec^{-1}$, lower panels) so to satisfy the constraint (12) that brings the system in the subthreshold regime.

An analogous set of cases, but with $\sigma^2 = 2.5\,mV^2msec^{-1}$, is shown in Fig. 3.

Both Figures show the presence of peaks at integer multiples of the period T_0. This confirms the ability of the system to detect the missing fundamental frequency despite its absence in the modulated stimulus. Peaks in the ISI distributions are produced also at integer multiples of the period $T_1 = \frac{2\pi}{f_1}$ which corresponds to the first harmonic component in the input term. For the higher value of the modulation amplitude A the peak height is increased in both cases with and without phase resetting. This behavior is maintained also for larger values of the noise intensity. The phase locking of spike generation times with the period T_0 is enhanced for smaller values of the noise intensity σ^2 (Fig. 2). The instantaneous resetting of the stimulus phases to their initial null values after the spikes produces more pronounced peaks and consequently deeper troughs among them in the ISI distribution. The composition of two harmonic terms generate constructive interferences at multiple of T_0 in the input signal and Fig. 2 and 3 illustrate how the response of the system to the stimulus preserves this property.

In Fig. 4, panels a and b, we compare the peak heights at T_0 for the parameter sets of Fig. 2 (bottom lines) and Fig. 3 (top lines) respectively, but for varying values of σ^2. In panels c and d we show the fraction of spikes occuring in the time interval $T_0 \pm 5\%$ as a function of the noise intensity σ^2.

The two measures capture the same characteristics of the considered phenomenon. All the curves shown pass through a maximum, thus confirming the arising of a resonance-like behavior. However only for the lower value of $A = 0.5\ mV\,ms^{-1}$ both the peak height at T_0 and the fraction of spikes produced around time T_0 reach such maximum within the range of σ^2 for which all the modeling and biological constraints are fulfilled (within bars in the Figures). Note that very small values of σ^2 become unadmissible since they correspond to
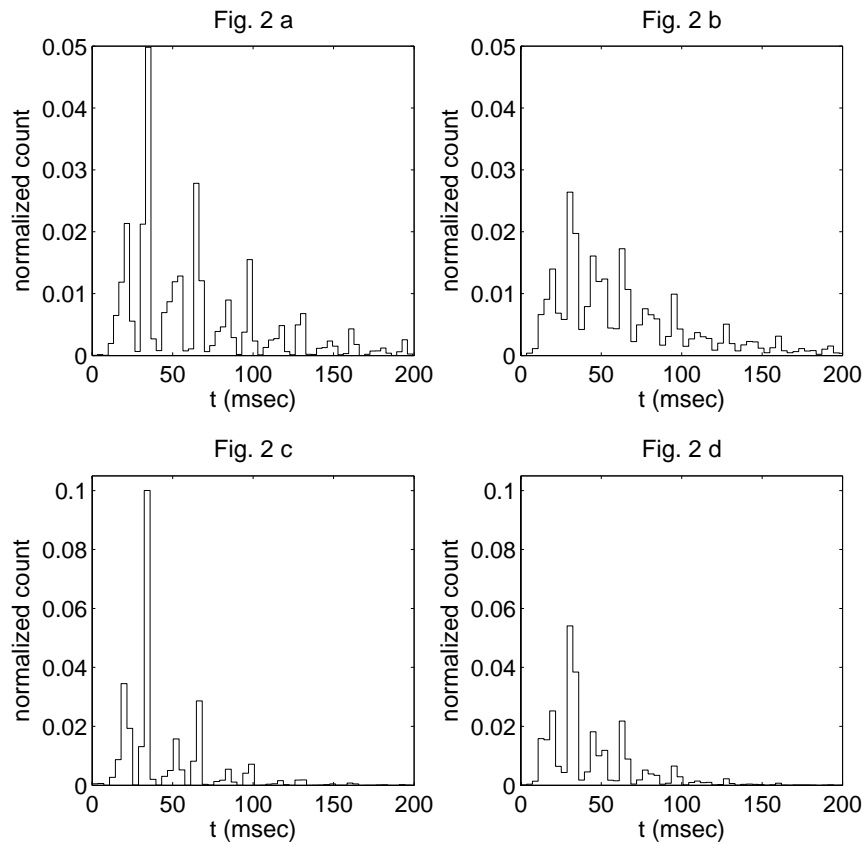
Figure 2: Histograms (panels a, c: case with phase reset) and normalized count plots (panels b, d: case without phase reset) of the ISI distributions for model (4) when $S = 10\,mV$, $\theta = 10\,msec$, $\mu = 0.6\,mV\,msec^{-1}$, $f_0 = 0.196349\,msec^{-1}$, $\sigma^2 = 0.9\,mV^2 msec^{-1}$ for $A = 0.5\,mV\,msec^{-1}$ (upper panels) and $A = 0.9\,mV\,msec^{-1}$ (lower panels). Here $T_0 \simeq 32\,msec$.
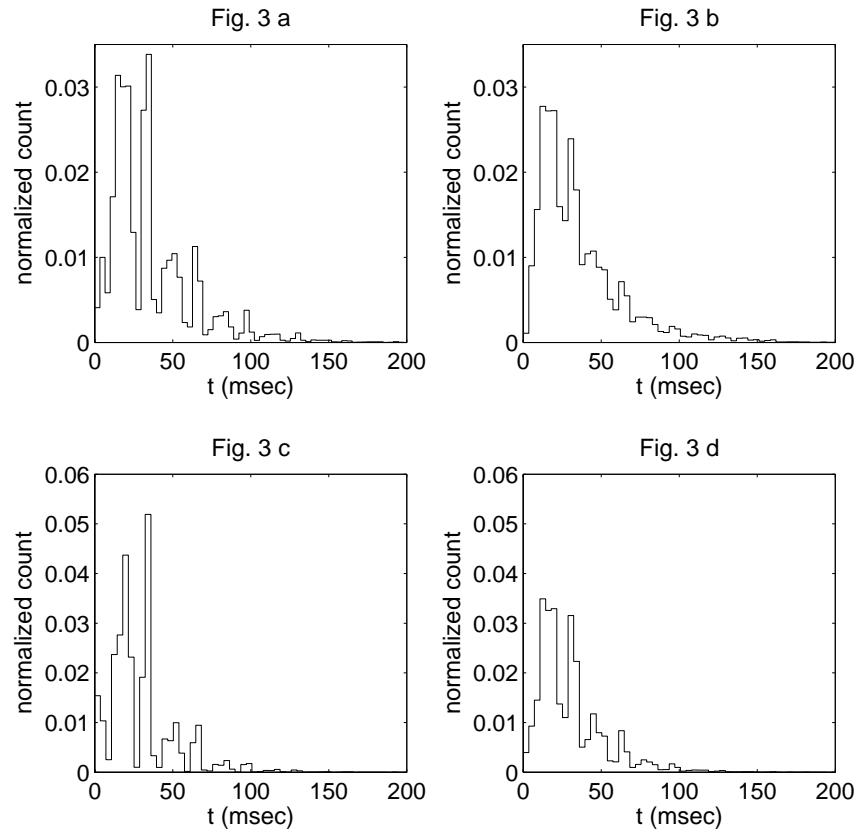
Figure 3: Histograms (panels *a*, *c*: case with phase reset) and normalized count plots (panels *b*, *d*: case without phase reset) of the ISI distributions for model (4) for the same parameter set as in Fig. 2, but with $\sigma^2 = 2.5\, mV^2 msec^{-1}$.
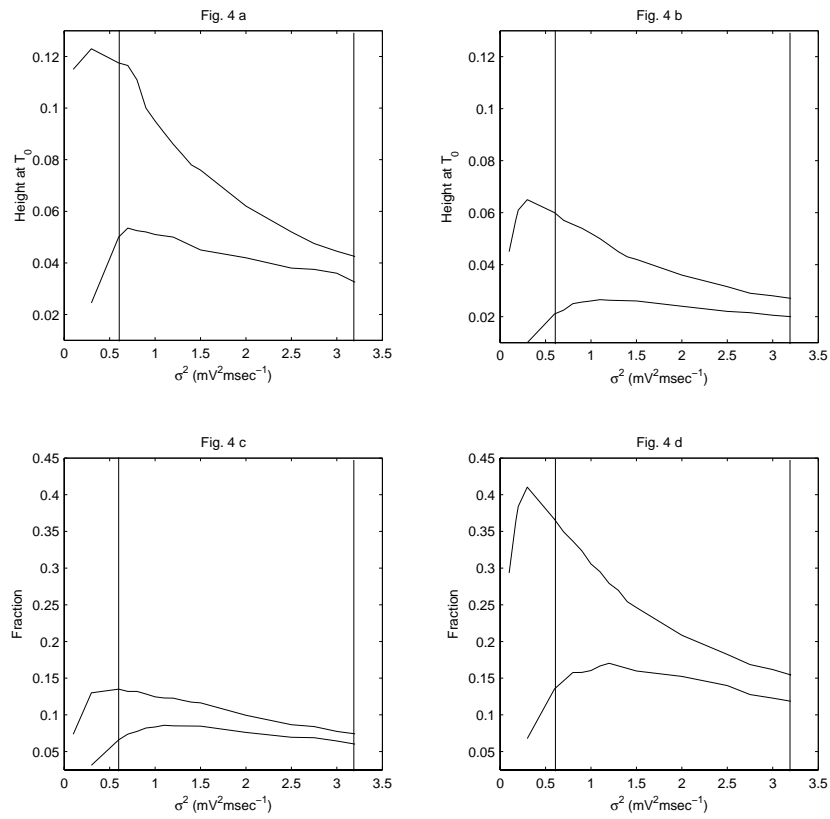
Figure 4: Height of the ISI distribution at T_0 (upper panels) and fraction of spikes at $T_0 \pm 5\%$ (lower panels) as a function of σ^2. Other parameters as in Fig. 2 with $A = 0.5 \, mV \, msec^{-1}$ (bottom lines), $A = 0.9 \, mV \, msec^{-1}$ (top lines). Vertical lines delimit the biologically admissible range.

too low spiking frequencies. The resonance-like behavior is enhanced as the modulation amplitude A is increased. Furthermore not resetting the phases of the stimulus after each spike implies that the heights of peaks are reduced while on the other hand the fraction of spikes around the time corresponding to the fundamental frequency are enhanced.

Framework (**2**). To gain insight into the dependence of the ISI distribution on the modulation frequencies we consider two values of T_0 that are respectively greater and smaller than the reference value $T_0 \simeq 32 \, msec$. Since from Fig. 4 the modulation amplitude $A = 0.5 \, mV \, ms^{-1}$ seems to optimize the stochastic resonance phenomenon we choose this value for the cases analyzed. In Fig. 5 we show the ISI distributions for the same parameter set as in Fig. 2, but with $T_0 = 15 \, msec$ and for noise levels $\sigma^2 = 0.9 \, mV^2 msec^{-1}$ and $\sigma^2 = 3.2 \, mV^2 msec^{-1}$ (upper and lower panels respectively). An analogous set of results, but in correspondence with a period $T_0 = 45 \, msec$, is shown in Fig. 6.
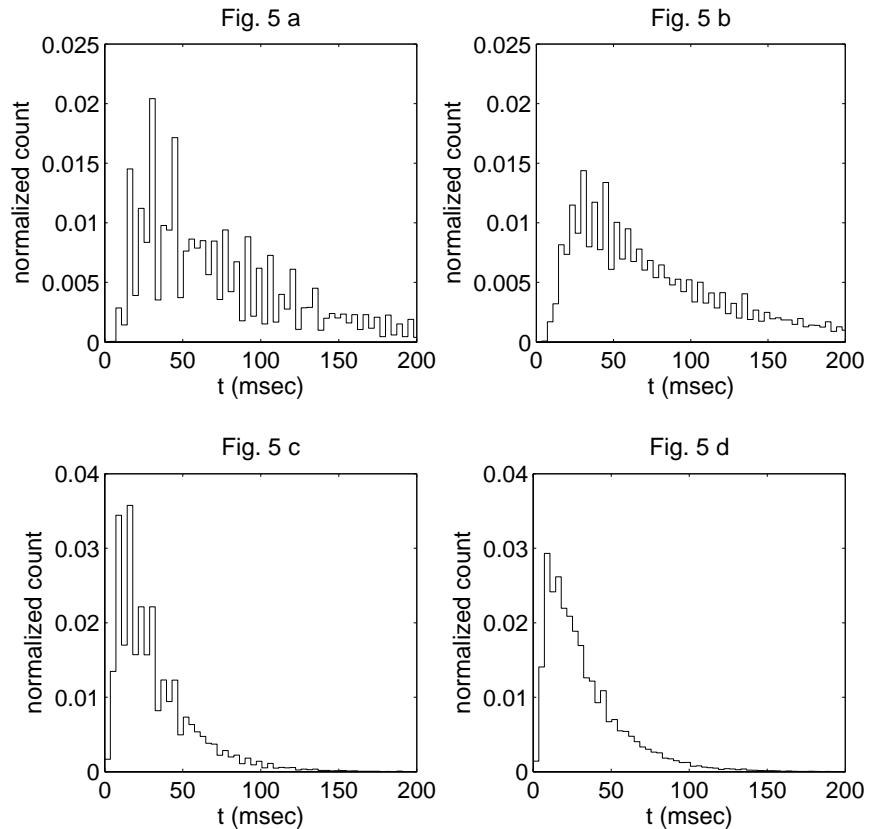
Figure 5: Histograms (panels *a*, *c*: case with phase reset) and normalized count plots (panels *b*, *d*: case without phase reset) of the ISI distributions for model (4) when $S = 10 \, mV$, $\theta = 10 \, msec$, $\mu = 0.6 \, mV \, msec^{-1}$, $f_0 = 0.418879 \, msec^{-1}$, $A = 0.5 \, mV msec^{-1}$ for $\sigma^2 = 0.9 \, mV^2 msec^{-1}$ (upper panels) and $\sigma^2 = 3.2 \, mV^2 msec^{-1}$ (lower panels). Here $T_0 \simeq 15 \, msec$.

The periods T_0 are set equal to 15 $msec$ and 45 $msec$ in order to consider values containing the mode of the ISI distribution in the absence of modulation if $\sigma^2 = 0.9 \, mV^2 msec^{-1}$.

Fig. 6 a

Fig. 6 b

Fig. 6 c

Fig. 6 d
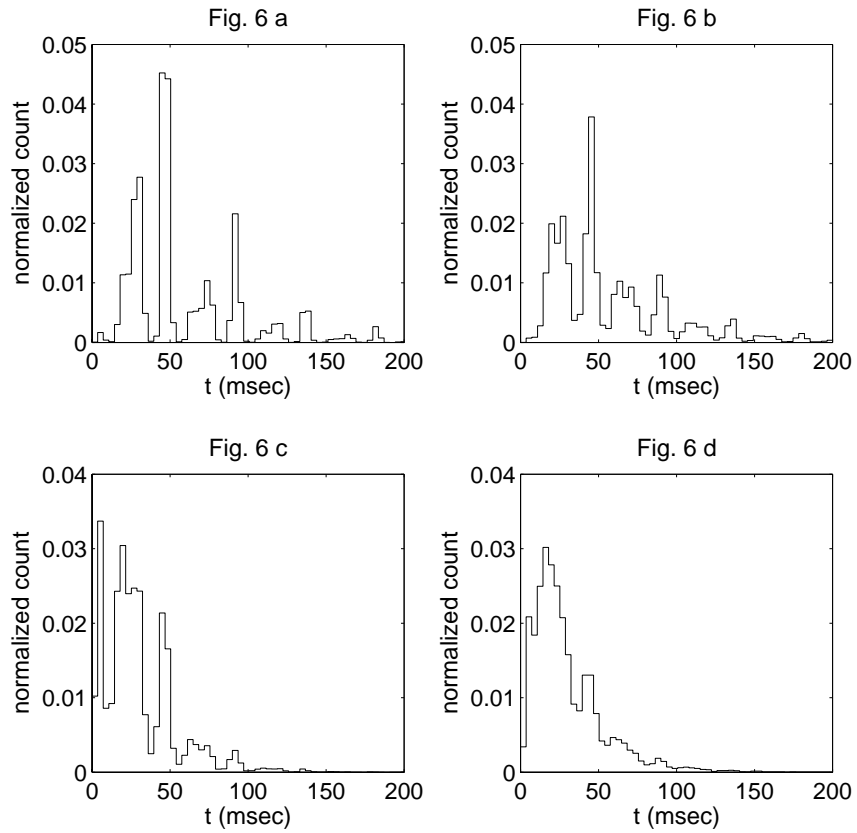
Figure 6: Same as in Fig. 5, but with $f_0 = 0.139626\,msec^{-1}$ corresponding to $T_0 \simeq 45\,msec$.

However for $\sigma^2 = 3.2 mV^2 msec^{-1}$ the mode falls around $12 msec$ which is less than both periods considered. The fundamental hidden frequency f_0 appears in all the Figures shown. The ghost frequency phenomenon is still present for the model described by (4) independently of the nearness of the fundamental frequency to the optimal one. However in correspondence with higher values of the period T_0 the response to the fundamental frequency becomes sharper. Shortest leading periods make the system perceive the modulation for a rather long time range, while for higher values of T_0 most of the probability mass in the distribution is concentrated over the first periods. Here again the peak heights at nT_0, $n = 1, 2, ...,$ in the ISI distribution are less pronounced and the trough depths is reduced when no resetting of the phases is performed.

In Fig. 7 we compare the peak heights of the ISI distribution at T_0 for the parameter sets of Fig. 5 and 6 (upper panels correspond to $T_0 = 15\ msec$, lower panels to $T_0 = 45\ msec$), but for varying σ^2.
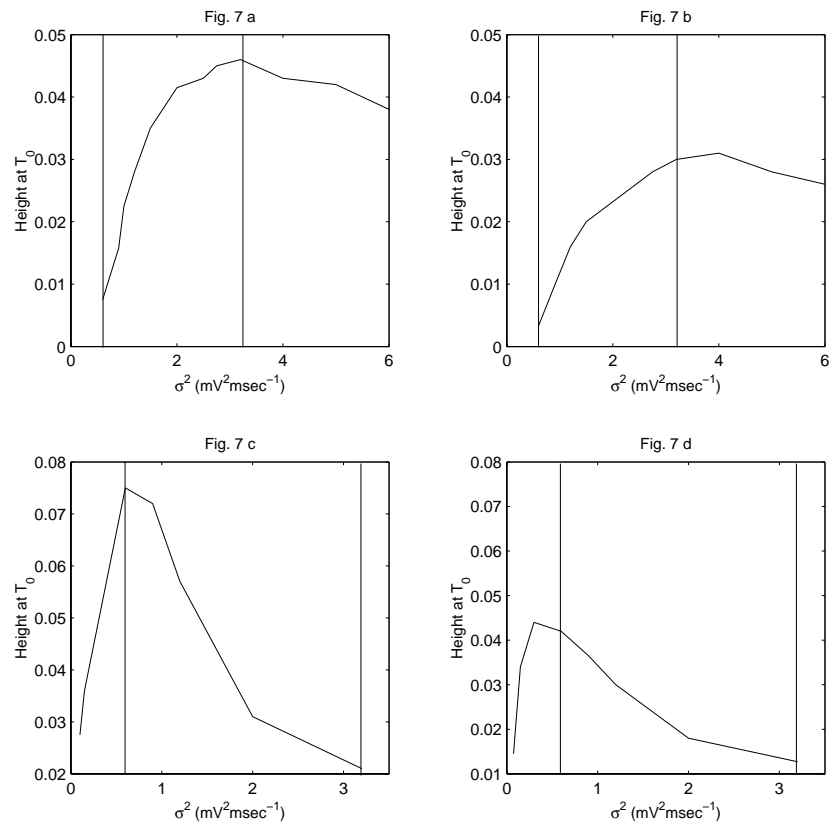
Figure 7: Height of the ISI distribution at T_0 as a function of σ^2 for the other parameters as in Fig. 5 (upper panels) and Fig. 6 (lower panels). Vertical lines delimit the biologically admissible range.

We do not show the plots for the fraction of spikes generated around T_0 since they simply confirm the previous results. In both cases stochastic resonance-like phenomena can be detected whereby the peak heights pass through a maximum as σ^2 is varied. However

the phenomenon is far more pronounced for $T_0 = 45\,msec$ while it is rather tied down if $T_0 = 15\,msec$. Furthermore the peak heights at T_0 reach their maxima in correspondence with noise levels that fall out of the range considered acceptable for the model neuron. In the case where $T_0 = 15\,msec$ this corresponds to considering very high firing frequencies with respect to the acceptable ones.

4   Conclusions We have investigated the response of a stochastic LIFM to a stimulus composed by the first two harmonics of a given fundamental frequency under both conditions where the input phases are reset or not to their initial null values after each occurrence of a spike.

The model solution to the SDE (4) has been shown to detect the ghost frequency and to exhibit a resonance-like behavior in correspondence with such frequency. The features illustrated by means of examples are common to a series of other cases that have been studied and are not reported in this work.

The model proposed is sufficiently complex to retain the main features of a stochastic Morris-Lecar one, but at the same time it is able to reproduce the properties discussed in (Chialvo (2002)) and (Chialvo (2003)) for a simpler neuronal model and to allow the same interpretation of the phenomena exhibited. However the results shown appear more easily understandable than for the Morris-Lecar model allowing to recognize the role of the composition of nonlinear features and randomness effects that produce the observed behaviors.

REFERENCES

[1] Arnold, L. (1974) *Stochastic Differential Equations: Theory and Applications.*, Wiley, New York.

[2] Balenzuela, P. and Garcia-Ojalvo, J. (2005) A neural mechanism for binaural pitch perception via ghost stochastic resonance. *Chaos* **15**(2): Art. No. 023903.

[3] Buldù J.M., Chialvo D.R., Mirasso C.R., Torrent M.C. and Garcia-Ojalvo J. (2003) Ghost resonance in a semiconductor laser with optical feedback. *Europhysics Letters* **64**(2): 178–184.

[4] Bulsara, A.R., Elston, T.C, Doering, C.R., Lowen, S.B. and Lindenberg, K. (1996) Cooperative behavior in periodically driven noisy integrate-fire models of neuronal dynamics. *Phys. Rev. E* **53**(4): 3958–3969.

[5] Buonocore, A., Nobile, A.G. and Ricciardi, L.M. (1987) A new integral equation for the evaluation of first-passage-time probability densities. *Adv. Appl. Prob.* **19**: 784–80.

[6] Chialvo, D.R., Calvo, O., Gonzales, D.L., Piro, O., Savino, G.V. (2002) Subharmonic stochastic synchronization and resonance in neuronal systems. *Phys. Rev. E* **65**(5): Art. No. 050902(R).

[7] Chialvo, D.R. (2003) How we hear what is not there: A neural mechanism for the missing fundamental illusion. *Chaos* **13**(4): 1226–1230.

[8] Calvo, O. and Chialvo, D.R. (2005) Ghost stochastic resonance in an electronic circuit. *Int. J. of Bifurcation and Chaos* : in press.

[9] Giraudo, M.T. and Sacerdote, L. (1999) An improved technique for the simulation of first passage times for diffusion processes. *Communication in Statistics: Simulation and Computation* **28**(4): 1135–1163.

[10] Kitajo, K., Nozaki, D., Ward, L.M and Yamamoto, Y. (2003) Behavioral stochastic resonance within the human brain. *Phys. Rev. Lett.* **90**(21): art. no.-218103.

[11] Lánský, P. (1997) Sources of periodical force in noisy integrate-and-fire models of neuronal dynamics. *Phys. Rev. E* **55**(2): 2040–2043.

[12] Lánský, P., Rodriguez, R. and Sacerdote, L. (2004) Mean instantaneous firing frequency is always higher than the firing rate. *Neural Computation* **16**: 477–489.

[13] Ricciardi, L.M., Di Crescenzo, A., Giorno, V. and Nobile, A.G. (1999) An outline of theoretical and algorithmic approaches to first passage time problems with application to biological modeling. *Math. Japonica* **50**(2): 247–322.

[14] Shimokawa, T., Pakdaman, K. and Sato, S. (1999) Time-scale matching in the response of a stochastic leaky integrate-and-fire neuron model to periodic stimulus with additive noise. *Phys. Rev. E* **59**(3): 3427–3443.

[15] Segundo, J., Vibert, J.-F., Pakdaman, K., Stiber, M., Diez Martinez, O. (1994) Noise and the neurosciences: A long history with a recent revival (and some theory). in *Origins: Brain & Self Organization* (K.H. Pribram Ed.), Lawrence Erlbaum, Hillsdale: 299–231.

[16] Tuckwell, H.C. (1988) *Introduction to theoretical neurobiology.*, Cambridge University Press.

[17] Victor, J.D. and Conte, M.M. (2000) Two-frequency analysis of interactions elicited by vernier stimuli. *Visual Neurosci.* **17**: 959–973.

[18] Wenning, G. and Obermayer, K. (2003) Activity Driven Adaptive Stochastic Resonance. *Phys. Rev. Let.* **90**(12): Art. No. 120602.

Maria Teresa Giraudo
DEPT. OF MATHEMATICS, UNIVERSITY OF TORINO
Via C. Alberto 10, 10123 Torino, Italy
E-mail: `mariateresa.giraudo@unito.it`

Laura Sacerdote
DEPT. OF MATHEMATICS, UNIVERSITY OF TORINO
Via C. Alberto 10, 10123 Torino, Italy
E-mail: `laura.sacerdote@unito.it`